Sensors and Materials, Vol. 35, No. 3 (2023) 989–999
MYU Tokyo

S & M 3223

Optimum Excitation Current of Fluxgate Based on Striped Array Iron Core

Zhijun Cui[1*] and Chen Liu[2]

[1]School of Electronic and Information Engineering, Ankang University, Ankang 725000, P. R. China
[2]School of Electronics and Information, Northwestern Polytechnical University, Xi'an 710129, P. R. China

(Received November 9, 2022; accepted January 10, 2023)

Keywords: fluxgate sensor, MEMS technology, optimum excitation current, striped array iron core

To reduce the power consumption of a micro-fluxgate, we propose the use of a striped array iron core, which reduces the demagnetization coefficient, to reduce the optimum excitation current of the micro-fluxgate. The power consumption is reduced since it is mainly determined by the optimum excitation current. The finite-element electromagnetic simulation software Magnet and the computing software MATLAB are used to jointly establish the fluxgate model to analyze the effect of the striped array iron core on the optimum excitation current of the micro-fluxgate, and the relationship between the structure of the striped array iron core and the optimum excitation current is obtained. Striped array iron cores with different structures are designed by micro-electromechanical technology. Finally, by comparing the experimental results with the simulation results, the validity of the simulation relationship is verified, which provides a theoretical and experimental basis for reducing the power consumption of the micro-fluxgate by changing the structure of the iron core.

1. Introduction

Magnetic field measurement, particularly weak magnetic field measurement, has long been a research direction in physics and engineering applications. A fluxgate is a measurement sensor for use in weak magnetic fields with good comprehensive performance.(1) It has a wide range of applications in aviation, aerospace, geophysics, and other fields requiring very high sensitivity and stability. In 1990, Thomas Seitz prepared the first micro-fluxgate using micro-electromechanical technology,(2) and the fluxgate, particularly the micro-fluxgate, is becoming an increasingly hot research topic worldwide. It is already possible to fabricate micro-fluxgates with a size of several square millimeters, and the problem of their large size has basically been solved. However, owing to the coil structure and saturation excitation mode of the fluxgate, the power consumption of the micro-fluxgate does not decrease significantly with the size reduction. Moreover, because the released heat is concentrated in a very small area, the heat dissipation of the micro-fluxgate is a serious challenge that directly threatens the thermal stability of the whole

*Corresponding author: e-mail: cuizj_163@163.com
https://doi.org/10.18494/SAM4242

ISSN 0914-4935

system.[3] Therefore, it is an urgent problem to reduce the power consumption of the micro-fluxgate.

The pulse excitation mode and excitation tuning method are commonly used to reduce fluxgate power consumption. Kubik *et al*.,[4] Drljaca *et al*.,[5] Ripka *et al*.,[6] Kubik *et al*.,[7] and Ponjavic and Veinovic[8] studied the pulse excitation technology of the fluxgate from different aspects. Through the use of this technology, the peak of the excitation current is kept constant and the width of the excitation pulse is reduced. However, pulse excitation technology reduces the sensitivity of the fluxgate and increases its noise. Belyayev and Ivchenko,[9] and Ripka and Hurley[10] used the excitation tuning method to reduce the power consumption of the fluxgate. In this method, a capacitor is connected in parallel or series in the excitation circuit, and the excitation circuit is allowed to resonate after the saturation of the iron core of the fluxgate by adjusting the capacitance. For the traditional structure fluxgate, the excitation tuning method can effectively reduce the power consumption without increasing the remanence error. However, this method is not suitable for the micro-fluxgate because the large coil resistance and planar structure make excitation tuning difficult.[9,10]

Both the pulse excitation mode and the excitation tuning method reduce the fluxgate power consumption through the external circuits, which cannot be applied to the micro-fluxgate. Liu used an iron core with a contracted structure to reduce the fluxgate power consumption.[11] Lv and Liu used an iron core with a porous structure to reduce the power consumption of the micro-fluxgate.[12] Therefore, optimizing the iron core structure of the micro-fluxgate is an effective method for reducing the power consumption.

In this paper, the finite-element simulation software Magnet and the calculation software MATLAB are used to establish a fluxgate model to analyze the effect of the striped array iron core on the optimum excitation current of the micro-fluxgate. In addition, the striped array iron cores with different structures are designed and fabricated by micro-electromechanical technology. By comparing the experimental and simulation results, the effectiveness of the simulation relationship is verified, which provides a theoretical and experimental basis for reducing the power consumption of the micro-fluxgate by changing the iron core topology.

2. Theoretical Analysis of Optimum Excitation Current

The fluxgate sensor is a kind of sensor used to measure the weak magnetic field that uses the nonlinear relationship between the magnetic induction intensity B and the magnetic field intensity H of the high-conductivity magnet iron core under the saturation excitation of the alternating magnetic field.[13]

The iron core performance for a low-power fluxgate is to ensure high permeability and low coercivity, and reduce the saturation field strength H_s as far as possible, so that the iron core can enter the saturation state with a small excitation current. In this way, the power consumption is effectively reduced while the sensitivity of the fluxgate is guaranteed.[14]

When the fluxgate of the closed magnetic circuit is excited by a sinusoidal current, the magnetic field $H_m \sin(wt)$ is generated in the iron core. If the external magnetic field is H_o, the amplitude of the second harmonic of the output voltage can be obtained as[11]

$$E_2 = -\frac{8}{3\pi} NS\mu\omega \frac{1}{H_m^2} \left\{ \left[H_m^2 - \left(H_s - H_o \right)^2 \right]^{\frac{3}{2}} - \left[H_m^2 - \left(H_s + H_o \right)^2 \right]^{\frac{3}{2}} \right\}, \tag{1}$$

where N is the number of turns of the detection coil, S is the cross-sectional area of the iron core, μ is the permeability of the iron core, and H_s is the intensity of the iron core saturation magnetic field.

To compare the power consumption of the fluxgate, the amplitude of the excitation magnetic field that maximizes the sensitivity of the fluxgate is defined as the optimum excitation magnetic field. The second harmonic sensitivity G_2 of the fluxgate is obtained by taking the derivative of Eq. (1) with respect to the external magnetic field H_o.

$$G_2 = \left. \frac{dE_2}{dH_o} \right|_{H_o = 0} = -\frac{16}{\pi} NS\mu\omega \frac{H_s}{H_m^2} \sqrt{H_m^2 - H_s^2} \tag{2}$$

In Eq. (2), the second harmonic sensitivity G_2 is equal to zero when H_m is equal to H_s or when H_m tends to ∞. It can be seen that there must be a value of H_m between H_s and ∞ that maximizes G_2. The amplitude of the optimum excitation magnetic field can be obtained as

$$H_{mb} = \sqrt{2} H_s. \tag{3}$$

At this time, G_2 reaches the maximum value, that is, the optimum sensitivity is obtained.

$$G_{2m} = -\frac{8}{\pi} NS\mu\omega \tag{4}$$

The current that produces the optimum excitation magnetic field inside the iron core of the fluxgate is defined as the optimum excitation current of the fluxgate. When the cross-sectional area of the iron core is fixed, the number of turns of the excitation coil is N_e, the length of the iron core is l, and the size of the excitation current is $i_e = I_m \sin(wt)$, considering the demagnetization effect of the iron core, the amplitude of the magnetic induction intensity of the iron core affected by demagnetization is

$$H_{m1} = \frac{1}{1 + D\left(\mu_r - 1 \right)} H_m = \frac{1}{1 + D\left(\mu_r - 1 \right)} \frac{N_e}{l} I_m. \tag{5}$$

Here, μ_r is the relative permeability of the iron core and D is the demagnetization factor. From this equation, we obtain

$$I_m = \frac{l}{N_e}\left[1 + D\left(\mu_r - 1\right)\right]H_{m1}. \tag{6}$$

When $H_{m1} < H_s$, μ_r is constant and high. When $H_{m1} > H_s$, $\mu_r = 1$. If $H_{m1} = \sqrt{2}\ H_s$, the amplitude of the optimum excitation current is

$$I_{m1} = \frac{l}{N_e}\left[1 + D\left(\mu_r - 1\right)\right]H_s + \frac{l}{N_e}\left[\sqrt{2}H_s - H_s\right] = \frac{l}{N_e}\sqrt{2}H_s + \frac{l}{N_e}D\left(\mu_r - 1\right)H_s. \tag{7}$$

According to Eq. (7), the optimum excitation current of the fluxgate consists of two terms. The first term is the excitation current required by the excitation coil to generate the optimum excitation magnetic field, which is only related to the size of the saturation magnetic field H_s of the iron core and the number of turns of the excitation coil. The second term is the extra excitation current required to overcome the demagnetizing field, which is related not only to the two factors in the first term, but also to the demagnetization coefficient and relative permeability of the iron core.

From the above analysis, it can be seen that the power consumption of the fluxgate is reduced by reducing the optimum excitation current. We should reduce the current value of the second term in Eq. (7) to reduce the optimum excitation current. By analyzing the factors affecting the second term, it can be seen that reducing the relative permeability μ_r can reduce the optimum excitation current, but it will also reduce the sensitivity of the fluxgate.[15] The saturation field strength H_s is mainly determined by the characteristics of magnetic materials and is not easy to decrease.[16] Therefore, the optimum excitation current can only be reduced by reducing the demagnetization coefficient D of the iron core, which is only related to the shape of the magnetic material.[17] Because D for the iron core is inversely proportional to the slenderness ratio of the iron core, a smaller cross-sectional area or a longer single iron core leads to a smaller D value for the iron core.[11] On this basis, the striped array iron core shown in Fig. 1 is adopted in this paper. When the total length of the iron core is constant, the cross-sectional area of each iron core in the striped array iron core is smaller than that of the thin film iron core of the traditional fluxgate. Therefore, the demagnetization coefficient of the whole striped array iron core is reduced. Finally, the aim of reducing the optimum excitation current of the fluxgate is achieved.

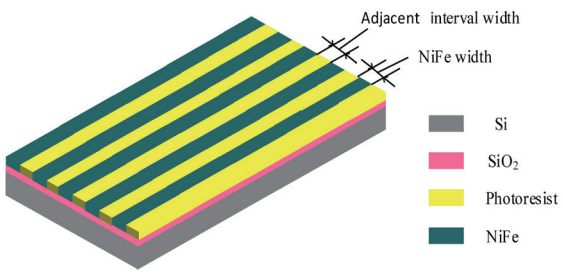

Fig. 1. (Color online) Schematic diagram of striped array iron core.

3. Simulation of Optimum Excitation Current of Striped Array Iron Core

To obtain the relationship between the size and density of the striped array iron core and the optimum excitation current, we used the finite-element simulation software Magnet and the computational software MATLAB to establish a fluxgate simulation model. The micro-fluxgate model is shown in Fig. 2. The excitation and detection coils on the striped array iron core are wound alternately. The excitation and detection coil parameters are shown in Table 1. The coil material is copper and $Ni_{82}Fe_{18}$ is selected as the iron core material in the simulation.

To explore the effect of the adjacent interval width of the striped array iron core on the optimum excitation current, we established micro-fluxgate models with five groups of striped array iron cores. The total thickness of the five groups of striped array iron cores is 1 μm, and the adjacent interval width of the striped array iron core is increased from 25 to 45 μm in 5 μm steps when the width of each iron core of the striped array iron core is 40 μm. The relationship between the magnetic flux of the detection coil and the excitation current is obtained using Magnet. In accordance with Faraday's law of electromagnetic induction, the output signal of the micro-fluxgate with five groups of striped array iron cores is calculated by using the induced magnetic flux variation. Finally, the optimum excitation current is obtained according to the amplitude of the output second harmonic signal under different excitation currents. The excitation current frequency is 1 kHz and the measured external magnetic field is 3 A/m in the simulation.

Figure 3 shows the relationship between the amplitude of the second harmonic of the fluxgate and the excitation current when the width of each iron core of the striped array iron core is 40 μm and the adjacent interval width of the striped array iron core is increased from 25 to 45 μm in 5 μm steps. First, the amplitude of the second harmonic of the fluxgate gradually increases with the excitation current. When the excitation current reaches a certain inflection point, the amplitude of the second harmonic of the fluxgate gradually decreases again. From the analysis of the optimum excitation current of the fluxgate, it is known that the current corresponding to

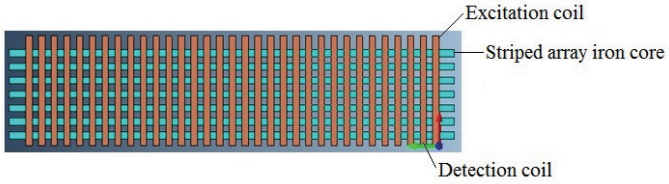

Fig. 2. (Color online) Micro-fluxgate 1/2 simulation model.

Table 1
Micro-fluxgate simulation model coil parameters.

Component	Length (μm)	Width (μm)	Thickness (μm)	Number of turns
Excitation coil	1000	40	1	40
Detection coil	1000	40	1	40

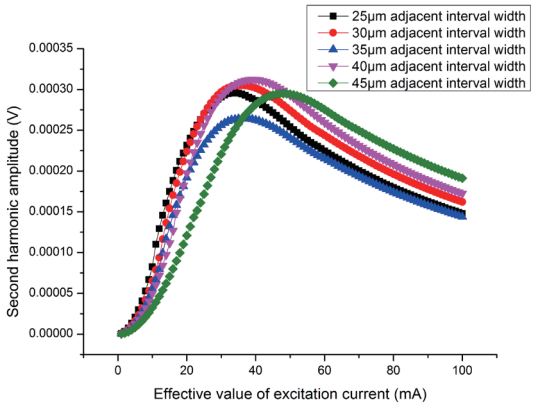

Fig. 3. (Color online) Relationship between the amplitude of the second harmonic and the excitation current (width of each iron core in striped array iron core of 40 μm).

this certain inflection point is the optimum excitation current of the fluxgate. In Fig. 3, the optimum excitation current value increases slowly with the adjacent interval width when the adjacent interval width of the striped array iron core is less than or equal to 35 μm, above which the optimum excitation current tends to increase suddenly.

To analyze the effect of the width of each iron core of the striped array iron core on the optimum excitation current of the fluxgate, we established micro-fluxgate models with seven groups of striped array iron cores. The striped array iron core retains the adjacent interval width of 40 μm and the total iron core thickness of 1 μm, and the width of each iron core of the striped array iron core is increased from 30 to 90 μm in 10 μm steps. The simulated excitation current frequency and the measured external magnetic field are maintained at 1 kHz and 3 A/m, respectively. The calculation method proposed in this section is adopted, and the relationship between the amplitude of the second harmonic of the striped array iron core and the excitation current for different widths of each iron core is obtained as shown in Fig. 4. The figure shows that the width of each core of the striped array iron core hardly affects the optimum excitation current size of the micro-fluxgate.

From the simulation results, it can be seen that adjusting the size and density of the striped array iron core will change the demagnetization coefficient of the striped array iron core. This affects the magnetic properties of the striped array iron core, thus changing its optimum excitation current. The optimum excitation current of the striped array iron core is hardly affected by changes in the width of each iron core, and the optimal excitation current of the fluxgate gradually increases with the adjacent interval width of the striped array iron core.

4. Optimum Excitation Current Test

4.1 Fabrication of striped array iron core

The electroplating of the striped array iron cores in this study was based on a micro-electromechanical system (MEMS) process, which was composed of photolithography and electroplating. The process of fabricating the striped array iron core is shown in Fig. 5. A 4-inch

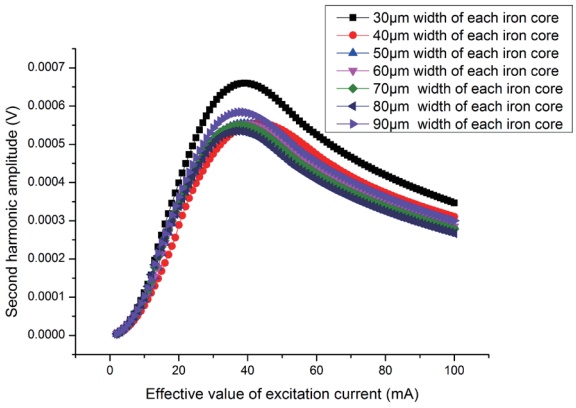

Fig. 4. (Color online) Relationship between the amplitude of the second harmonic and the excitation current (adjacent interval width of striped array iron core of 40 μm).

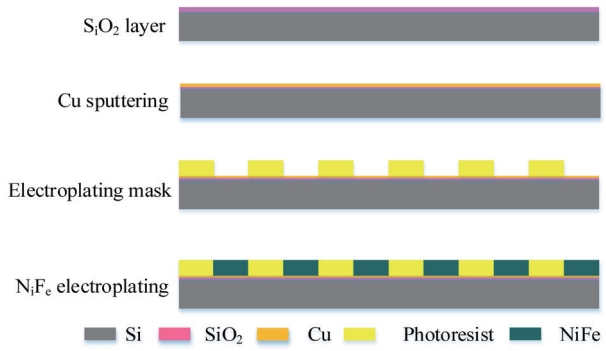

Fig. 5. (Color online) Process of fabricating the striped array iron core.

silicon wafer of 500 μm thickness was used as the substrate, and a 300-nm-thick SiO_2 layer was first deposited on its surface by wet oxygen oxidation as an insulating layer. Secondly, a Cu seed layer of 90 nm thickness was deposited on the SiO_2 layer by magnetron sputtering. During the sputtering, the substrate was kept at 200 °C to increase the adhesion between the Cu seed layer and the substrate. Thirdly, the photoresist (EPG533) of 1.5 μm thickness was spin-coated on the Cu seed layer, and the mask of the electroplated striped array iron core was fabricated by photolithography. Finally, the striped array iron core was fabricated by electroplating with the mask of the striped array iron core.

During the electroplating, the direct current density was set as 3 A/dm^2 for 3 min, the width of each iron core in the striped array iron core was varied from 30 to 90 μm in 10 μm steps, and the adjacent interval width of the striped array iron core was increased from 25 to 45 μm in 5 μm steps. There were 35 groups of striped array iron cores considered in this study. The total thickness of the striped array cores was measured to be about 1 μm using a DektakXT step analyzer. One of the striped array iron core samples fabricated by electroplating is shown in Fig. 6 (the width of each iron core in the striped array iron core is 60 μm and the adjacent interval width of the striped array iron core is 25 μm).

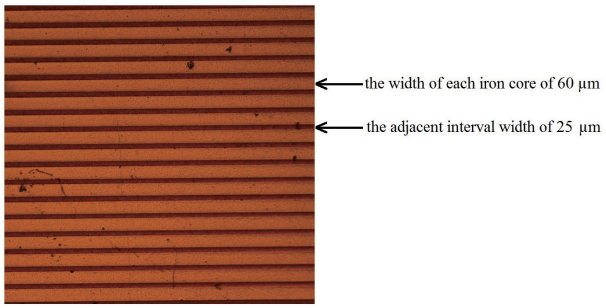

Fig. 6. (Color online) SEM image of fabricated striped array iron core with width of each iron core of 60 μm and adjacent interval width of 25 μm.

4.2 Optimum excitation current test

We created a measurement system to measure the optimum excitation current of the flat-structure fluxgate composed of striped array iron cores prepared by electroplating. The principle of the measurement system is shown in Fig. 7. The excitation signal of the fluxgate was generated by cascading a signal generator (Agilent 33220A) and a power amplifier (NFHSA 4011). An amperometer (Agilent 34401A) was placed in series with the excitation circuit to measure the excitation current.

A DC power supply (Agilent E3610A) drove the solenoid to generate an external magnetic field while the excitation current was measured using the amperometer. An oscilloscope (Agilent Oscilloscope Infiniium 54830D) or a spectrum analyzer (Tektronix RSA 5103A) was connected to detection coils to measure and analyze the output voltage signal of the fluxgate. The excitation current frequency was 1 kHz and the measured external magnetic field was 3 A/m when the optimum excitation current of 35 groups of striped array iron cores prepared by electroplating was tested.

A magnetic shielding device was used to exclude the effect of the geomagnetic field in the measurement of the fluxgate to simulate the zero magnetic field space in an actual measurement.

Using the measurement system shown in Fig. 7, the optimum excitation current properties of the 35 groups of striped array iron cores were measured and are shown in Fig. 8.

5. Results and Discussion

The optimum excitation current test results of the 35 groups of striped array iron cores are shown in Fig. 8. It can be seen that the optimum excitation current increases slowly with the width of each iron core of the striped array iron core when the adjacent interval width in the striped array iron core is unchanged. Because the magnetic properties of $Ni_{82}Fe_{18}$ used as the iron core material in the simulation are more ideal than those used in practice, the optimum excitation current test results are slightly different from the simulation results when the adjacent interval width in the striped array iron core is unchanged. The optimum excitation current

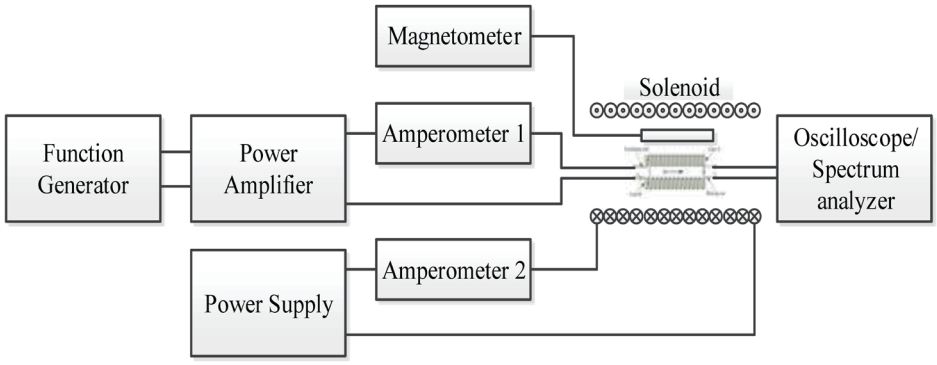

Fig. 7. Principle of system for measuring the optimum excitation current properties of the micro-fluxgate.

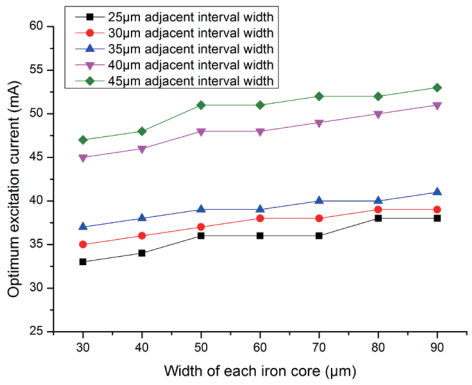

Fig. 8. (Color online) Optimum excitation current of striped array iron cores.

increases with the adjacent width of the striped array iron core when the width of each iron core of the striped array iron core is unchanged. The optimum excitation current is relatively small when the adjacent interval width in the striped array iron core is less than or equal to 35 μm but starts to increase suddenly when it increases to 40 μm. The optimum excitation current changes with the same trend as that for the increasing width of each iron core of the striped array iron core when the adjacent width of the striped array iron core is greater than or equal to 40 μm.

In the field of micromagnetism, the magnetostatic coupling effect between the striped array iron cores for the adjacent interval width of 35 μm is stronger than that for the adjacent interval width of 40 μm. This magnetostatic coupling effect is beneficial for weakening the demagnetic field generated by each iron core of the striped array iron core during magnetization.[18] Therefore, the optimal excitation current for the adjacent interval width of 40 μm varies sharply than that for the adjacent interval width of 35μm with the width of each iron core of the striped array iron core as shown in Fig. 8.

The comparison between experimental and simulation results of the optimum excitation current with different adjacent interval widths of the striped array iron core is shown in Fig. 9 for

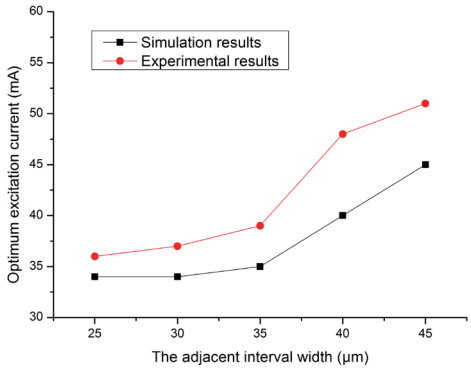

Fig. 9. (Color online) Comparison between experimental and simulation results of optimum excitation current (width of each iron core in striped array iron core of 40 μm).

the width of each iron core of the striped array iron core of 40 μm. It can be seen that the optimum excitation current of the striped array iron core increases slowly with the adjacent interval width in both the experimental test and the simulation when the adjacent interval width is less than or equal to 35 μm, but it increases suddenly above this width.

The relationship between the optimum excitation current of the striped array iron cores and the adjacent interval width of the striped array iron cores originated from the magnetostatic coupling effect between the striped array iron cores. This magnetostatic coupling effect between the striped array iron cores decreased with the increase in the adjacent interval width of the striped array iron core when the width of each iron core of the striped array iron core was unchanged, and the magnetostatic coupling effect was observed to be beneficial for eliminating the demagnetic field generated by each iron core of the striped array iron core during magnetization.[18]

Because there will be some interference of the weak magnetic field during the experimental test, the experimental result curve is slightly higher than the simulation result curve. However, the overall trend is basically the same for the experimental and simulation results of the optimum excitation current and does not affect the selection of the optimum model of the striped array iron core.

6. Conclusions

In this paper, we proposed a striped array iron core to reduce the optimum excitation current of a micro-fluxgate by reducing the demagnetization coefficient, so as to reduce the power consumption of the micro-fluxgate. A simulation model of the fluxgate was established using Magnet, and the effect of the striped array iron core on the optimum excitation current of the micro-fluxgate was analyzed. The relationship between the size and density of the striped array iron core and the optimum excitation current was obtained. The design and fabrication of the striped array iron cores with different structures were carried out by micro-electromechanical technology. By comparing the experimental results with the simulation results, the validity of the simulation relationship was verified, providing a strong theoretical and experimental basis for further designing the micro-fluxgate from the iron core structure to reduce the power consumption.

Acknowledgments

This work was supported by the Fundamental Research Funds for the National Natural Science Foundation of China (No. 61801005), the Natural Science Foundation of Shaanxi Province (No. 2022JM-391), and the Science and Technology in Ankang Project (No. AK2022-GY-08) .

References

1 P. Ripka and S. W. Billingsley: IEEE Trans. Magn. **34** (1998) 1303. https://doi.org/10.1109/20.706529
2 T. Seitz: Sens. Actuators, A **22** (1990) 779. https://doi.org/10.1016/0924-4247(89)80081-0
3 J. Kubik, L. Pavel, and P. Ripka: Sens. Actuators, A **130**–**131** (2006) 184. https://doi.org/10.1016/j.sna.2005.12.027
4 J. Kubik, L. Pavel, P. Ripka, and P. Kaspar: J. Sens. **10** (2005) 432. https://doi.org/10.1109/ICSENS.2005.1597728
5 P. M. Drljaca, P. Kejik, F. Vincent, D. Piguet, and R. S. Popovic: IEEE Sens. J. **5** (2005) 909. https://doi.org/10.1109/JSEN.2004.840836
6 P. Ripka, S. O. Choi, A. Tipek, S. Kawahito, and M. Ishida: IEEE Trans. Magn. **37** (2001) 1998. https://doi.org/10.1109/20.951033
7 J. Kubik, L. Pavel, P. Ripka, and P. Kaspar: IEEE Sens. J. **7** (2007) 179. https://doi.org/10.1109/JSEN.2006.886998
8 M. Ponjavic and S. Veinovic: J. Magn. Magn. Mater. **518** (2021) 167368-1. https://doi.org/10.1016/j.jmmm.2020.167368
9 S. Belyayev and N. Ivchenko: Meas. Sci. Technol. **29** (2018) 045008-1. https://doi.org/10.1088/1361-6501/aaa27e
10 P. Ripka and W. G. Hurley: Sens. Actuators, A **129** (2006) 75. https://doi.org/10.1016/j.sna.2005.09.047
11 S. B. Liu: Sens. Actuators, A **130**–**131** (2006) 124. https://doi.org/10.1016/j.sna.2005.12.004
12 H. Lv and S. B. Liu: J. Nanosci. Nanotechnol. **16** (2016) 2663. https://doi.org/10.1166/jnn.2016.10773
13 S. R. Wei, X. Q. Liao, H. Zhang, and J. H. Pang: Sensors **21** (2021) 1500. https://doi.org/10.3390/s21041500
14 P. M. Wu and C. H. Aho: IEEE Trans. Magn. **43** (2007) 1040. https://doi.org/10.1109/TMAG.2006.888640
15 Z. Y. Luo, J. Tang, B. Ma, Z. Z. Zhang, Q. Y. Jin, and J. P. Wang: Chin. Phys. Lett. **29** (2012) 456. https://doi.org/10.1088/0256-307X/29/12/127501
16 F. Primdahl, B. Hernando, O. V. Nielsen, and J. R. Petersen: J. Phys. E: Sci. Instrum. **22** (1989) 1004. https://doi.org/10.1088/0022-3735/22/12/009
17 Y. Z. Wang, S. J. Wu, Z. J. Zhou, D. F. Cheng, N. Pang, and Y. X. Wan: J. Sens. **13** (2013) 11539. https://doi.org/10.3390/s130911539
18 J. Velázquez, C. García, M. Vázquez, and A. Hernando: Phys. Rev. B **54** (1996) 9903. https://doi.org/10.1103/PhysRevB.54.9903